Convective mass transport in porous sloping layers

Arild Ludvigsen [1], Enok Palm [2], Robert Mc Kibbin [3]

[1]Departments of Mathematics, Section of Mechanics, University of Oslo, Blindern, Norway

[2]Departments of Mathematics, Section of Mechanics, University of Oslo, Blindern, Norway

[3]Department of Engineering Science, University of Auckland, Privat Bag, Auckland, New Zealand.

Abstract

Natural convection, caused by non - horizontal isolines for water density in sloping sandstone layers, is studied. The flow field is calculated for a fluid filled three - layer model composed of two identical sandstone strata separated by a low permeability layer (shale). The condition for resirculation within the sandstone is found. It is shown that, for layers of sufficiently small aspect ratio, the shale layer has negligible effect on the flow.

With the assumption that the fluid density is a function only of temperature, the effect of the flow on the change of porosity in the sandstone layers is examined. The spatial change of porosity is calculated for small values of time. It is shown that the maximum change takes place at the midpoints of the endwalls if the angle between the isotherms and the slab is less than 36.5^0, and at the midpoint of the lateral boundaries when this angle is greater than 36.5^0. Also discussed is how the angle the isotherms make with the horizontal depends on the thermal conductivities of the sandstone layers and the bounding rock.

1. Introduction

The study of diagenetic prosesses in sedimentary basins is of great importance in connection with oil - basin analyses. The diagenetic processes involve reactions between porewater and mineral phases. The solubility of the common mineral phases like quartz is a function of temperature and dissolution and temperature may therefore result from advection. Changes in porosity and permeability due to dissolution and precipitation of minerals will depend strongly on the transport of minerals while in solution.

If the porewater is almost stationary, the transport of dissolved ions will be limited to diffusion. Normally, however, porewater is not stationary relative to the sedimentary structure. Different types of water flow which may occur in sediments are mentioned in an article by Bjørlykke, Mo & Palm (1988) - meteoric water driven by a hydrostatic head, porewater flow driven by gradual compaction and porewater flow driven by differences in the density of the fluid (thermal convection and salinity driven flow) are discussed.

The last type of flow is due to (i) instability caused by the density of water increasing with height, or (ii) the isolines for density of water being non - horizontal. In the former case the increase of density with height is usually due to heat transport upwards, and may be modified by salinity effects. This kind of free convection taking place in a porous medium is called Rayleigh - Darcy convection, or just Rayleigh convection. The conditions for Rayleigh convection to occur in sedimentary layers have recently been discussed by Bjørlykke, Mo & Palm (1988) and Palm (1990).

In the first article a model composed of three horizontal layers is studied. The lowest and uppermost layers were supposed to be of sandstone with high permeability and a middle layer of shale with a low permeability. It was shown, by calculating the flow lines, that even very thin layers ($< 1m$) with low permeability would split potentially large convection cells into smaller units of clean sandstone beds which may then be too small to exceed the critical Rayleigh number.

In the second paper (Palm 1990), the necessary thickness of the individual clean sandstone beds for Rayleigh convection to take place and the subsequent change in porosity are calculated for realistic boundary conditions and values of the various parameters. Using permeabilities as high as 5 and 10 Darcies, it is found that the sandstone layer must be 30 - 60 m thick; this

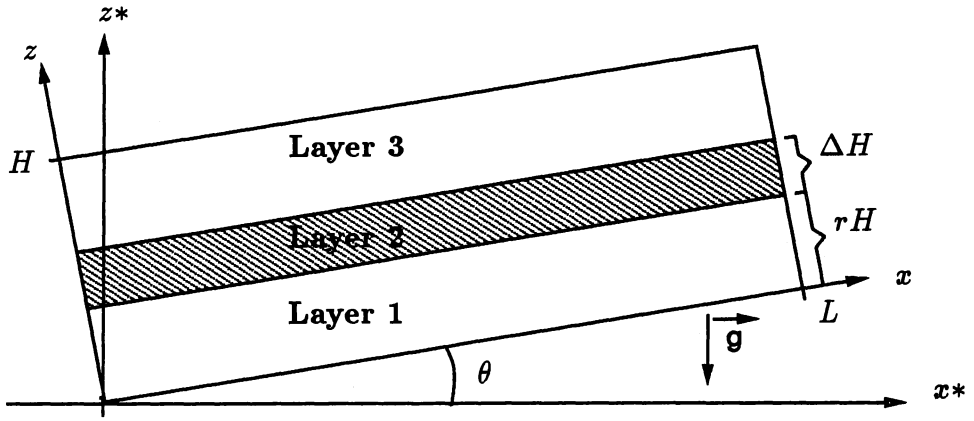

Figure 1.1: The symmetrical three-layer system. The thickness and length of the matrix is H and L, respectively. The thickness of the middle layer is ΔH. A coordinate system with axes parallel with the layer boundaries is introduced. The layers make an angle θ with the horizontal.

condition is rarely met in sedimentary basins.

The present paper is concerned with the second kind of convection: forced convection in sedimentary layers caused by non - horizontal isolines for the water density. Whereas it is likely that Rayleigh convection occurs rarely in sedimentary layers, the second kind of convection always takes place, given that the density isolines are non - horizontal. For this problem it is common to assume that the fluid density is a function only of temperature, and that the isotherms are parallel to the lateral walls i.e. perpendicular to the end - walls. The motion in this model has been studied both theoretically and experimentally by Bories & Combarnous (1973). They found that for moderate values of the temperature difference between the lateral boundaries, the motion is a unicellular flow (as in figure 4.2 (a) of this paper). If, however, the temperature difference is increased above a certain value, the unicellular flow becomes unstable and Rayleigh convection occurs (also see Palm 1990). In the present study it is assumed that the temperature difference is so small that Rayleigh convection does not occur; this is a realistic asumption for the physical problem examined here.

Two different aspects of the problem will be discussed in this paper. It was mentioned above that even very thin low - permeability layers may prevent Rayleigh convection to be set up. The first aspect studied here is the effect of strata of low permeability on convection in sloping porous layers. A three - layer model is considered, composed of two identical layers of sandstone with a thin shale layer between. Clearly the low - permeability layer cannot totally prevent a convective flow if the water density isolines are inclined to the horizontal. However, the layer may cause separation of the streamlines

in the sandstone layers, thereby leading to resirculation and a reduction in the strength of the water flow.

The aspect ratio $b = H/L$ (see figure 1.1) is very small. It then seems reasonable that, far from the end walls, the motion is independent of the $x-$ coordinate. It follows (equation(3.2)) that $\partial u/\partial z$ (u is the velocity in the x - direction) is known in all three layers and then that u is a known function of z. It turns out, however, that when resirculation occurs in the sandstone layers, the velocity w (in the z - direction) in the middle layer is not independent of x, even for very small aspect ratios. To solve this problem, it is therefore necessary to take the effect of endwalls into account.

It will be shown that whether resirculation within the sandstone layers occurs or not depends on the value of q/b^2, where $q = K_2/K_1$ with K_2 denoting the permeability of the thin shale layer and K_1 that of the thicker sandstone strata. If $q/b^2 \leq 1$, resirculation will occur and the effect of the thin shale layer is important. If $q/b^2 >> 1$, the effect of the shale layer is negligible. Hence, if K_1 and K_2 have known values and b is sufficiently small, the motion far from the end walls will not be influenced by the existence of thin shale layers.

The second problem which is discussed is the transport of dissolved materials and consequent changes in the porosity. For simplicity, only a single - layer sandstone model is studied. It is assumed that the isolines for water density make an angle γ with the horizontal, and that this may be different from the angle θ which the sandstone slab makes. It is shown that the maximum change in porosity occurs at the mid - points of the end walls if $\theta - \gamma$ is less than 36.5^0 and at the midpoints of the lateral boundaries if $\theta - \gamma$ is larger than 36.5^0.

2. The mathematical model

The conceptual model studied is the configuration shown schemathically in figure 1.1, consisting of a three layer permeable slab of thickness H making an angle θ with the horizontal. The upper and lower layers are identical, each having a uniform isotropic permeability $K = K_1$. The middle stratum has a smaller permeability, $K = K_2$, and thickness ΔH. The thicknesses of the upper and lower layers are each denoted rH where,

$$r = \frac{1}{2}\left(1 - \frac{\Delta H}{H}\right) \tag{2.1}$$

The layers are all assumed to be saturated with liquid water, with a flow that is two - dimensional and steady (independent of time). The fluid flow rate is described by the Darcy velocity, or mean specific discharge, $\vec{v} = (u, w)$ where $u(x, z)$ and $w(x, z)$ are the components in the x and z directions, respectively. It is assumed that the fluid flow can be described by the Rayleigh - Darcy equations. Applying the Boussinesque approximation (i.e. density variations is important only in the buoyancy terms), these equations may be written:

$$\frac{\partial u}{\partial x} + \frac{\partial w}{\partial z} = 0 \tag{2.2}$$

$$\vec{v} = \frac{K}{\mu}(-\nabla p + \rho \vec{g}) \tag{2.3}$$

$$u\frac{\partial T}{\partial x} + w\frac{\partial T}{\partial z} = \kappa \nabla^2 T \tag{2.4}$$

$$u\frac{\partial S}{\partial x} + w\frac{\partial S}{\partial z} = \kappa_s \nabla^2 S \tag{2.5}$$

$$\rho = \rho_0[1 - \alpha(T - T_0) + \alpha_s(S - S_0)] \tag{2.6}$$

where (2.2) - (2.5) are the equations of continuity, conservation of momentum (Darcy's law), thermal energy and salinity respectively while (2.6) is the equation of state which describes how the fluid density ρ changes with temperature T and salinity S. Here p is the fluid pressure, T_0 and S_0 are a reference temperature and a reference salinity, ρ_0 is the density at the values T_0, S_0. α is the coefficient of thermal expansion, α_s is the specific density change coefficient for salinity, κ is the thermal diffusivity for the saturated porous medium and κ_s is the diffusivity of salt in water. The dynamic viscosity of the fluid is μ (assumed constant), while $\vec{g}$ is the gravitational acceleration.

We introduce a stream function $\psi(x, z)$ defined by

$$u = \frac{\partial \psi}{\partial z}, \quad w = -\frac{\partial \psi}{\partial x} \tag{2.7}$$

and which identically satisfies (2.2). Subsequent elimination of p using (2.3) gives:

$$\nabla^2 \psi = \frac{gK}{\mu} \frac{\partial \rho}{\partial x^*} \tag{2.8}$$

where x^* is the horizontal coordinate (see figure 1.1).

Now, from (2.6), the fluid density ρ is a function of temperature and salinity. In studies of problems similar to that beeing investigated here, it is usual to assume that the temperature is constant at the boundaries $z = 0$ and $z = H$. However, observations in sedimentary layers show that the isotherms usually make an angle with the horizontal that is considerably smaller than that made by sloping geological structure. It is also clear that the velocity of the pore water flow in sedimentary basins is very small.

As a first approximation, then, we assume that the temperature and salinity are determined mainly by diffusion processes and, in accordance with observations, assume that the isotherms and salinity isolines make angles γ and γ_s with the horizontal; these angles are fixed and, to the present approximation, are independent of the fluid velocity. They are also not necessarily equal to θ, the angle of the layers.

In higher - order approximations, when convective effects are also taken into account, the boundary conditions determine the temperature and salinity distributions. Here, however, we do not need these higher - order terms.

We therefore write

$$T = T_0 + T_d(x, z) + T_c(x, z) \tag{2.9}$$

$$S = S_0 + S_d(x, z) + S_c(x, z) \tag{2.10}$$

where T_d and S_d are the solutions of the respective diffusion equations and T_c and S_c are the (negligible) contributions due to convective processes. From (2.4) and (2.5),

$$\nabla^2 T_d = 0 \tag{2.11}$$

$$\nabla^2 S_d = 0 \tag{2.12}$$

with solutions of the form

$$T_d = ax^* - bz^* + c \tag{2.13}$$

$$S_d = a_s x^* - b_s z^* + c_s \tag{2.14}$$

where x^* and z^* are horizontal and vertical coordinates respectively, and also $a/b = \tan\gamma$ and $a_s/b_s = \tan\gamma_s$; c and c_s are constants.

Introducing (2.6) into (2.8) and replacing T and S with T_0+T_d and S_0+S_d respectively, we obtain

$$\nabla^2\psi = -\frac{\alpha g K}{\nu}|\nabla T_d|\sin\gamma + \frac{\alpha_s g K}{\nu}|\nabla S_d|\sin\gamma_s \tag{2.15}$$

where $K = K_1$ in the upper and lower layers, $K = K_2$ in the middle layer and $\nu = \mu/\rho_0$. The terms $|\nabla T_d|$ and $|\nabla S_d|$ are the constant absolute values of the gradients of the (known) first approximations to the temperature and salinity distributions respectively.

It will be shown that the slope of the isotherms, $\tan\gamma$, is determined by the value of the thermal conductivity, k, of the rock layers (the middle layer is assumed to have the same conductivity as the sandstone) and that of the boundary rock, k_s. The aspect ratio $b = H/L$ (see figure 1.1) is assumed small and heat transfer far from the endwalls is considered. The boundary rock consists of upper surroundings ($z > H$) and lower surroundings ($z < 0$). At large negative values of the vertical coordinate z^*, it is assumed that the heat transport Q is uniform and given by $Q = k_s dT/dz^*$. The solution of (2.11) fulfilling this boundary condition, together with the requirement of conservation of heat flow and temperature at $z = 0$ and $z = H$ is

$$z > H: \qquad T_d = -\frac{Q}{k_s}z^* + c_1 \tag{2.16}$$

$$0 < z < H: \quad T_d = -\frac{\alpha Q}{k}z^* + \frac{\beta Q}{k}x^* + c_2 \tag{2.17}$$

$$z < 0: \qquad T_d = -\frac{Q}{k_s}z^* + c_3 \tag{2.18}$$

where

$$\alpha = \frac{1 + \frac{k}{k_s}\tan^2\theta}{1 + \tan^2\theta} \tag{2.19}$$

$$\beta = \frac{(1 - \frac{k}{k_s})\tan\theta}{1 + \tan^2\theta} \tag{2.20}$$

To evaluate c_1, c_2 and c_3 one more boundary condition is needed; for example, the temperature at a certain value of z^* in the upper or lower surroundings. However, we do not need these constants to determine the value of $\tan\gamma$. From (2.13), (2.17), (2.19) and (2.20), it is finally found that

$$\tan\gamma = \frac{a}{b} = \frac{\beta}{\alpha} = \frac{(1 - \frac{k}{k_s})\tan\theta}{1 + \frac{k}{k_s}\tan^2\theta} \tag{2.21}$$

which gives $\tan\gamma$ as a function of k/k_s and $\tan\theta$. The following properties of the relation (2.21) are immediately observed:

1. When $k = k_s$, i.e. the conductivities of the sandstone and surrounding rock are the same, the isotherms are horizontal. This is an obvious result.

2. For $k/k_s < 1$, $\tan\gamma$ has the same sign as $\tan\theta$. For $k/k_s > 1$, $\tan\gamma$ and $\tan\theta$ have opposite signs.

3. When $k << k_s$, $\tan\gamma \approx \tan\theta$.

These results and a formula for the isotherms were derived by Davis et al. (1985) , who considered the more general problem where the sand layer had curvature. They therefore had to assume that the slope of the layer, θ, is small (as well as the aspect ratio). That assumption is not made here. In the examples in Section 5, then, finite values of θ can be considered.

Similarly, a formula for the slope of the isolines for salinity may be obtained. This leads to finding $\tan\gamma_s$ as a function of $\tan\theta$ and the diffusivity for salt in water.

3. Non - dimensionalisation and solution method

Using a length scale H, the thickness of the layered slab, dimensionless co-ordinates are $X = x/H$ and $Z = z/H$. A non dimensional streamfunction $\psi(x, z)$ is given by

$$\psi = \Psi/\kappa \tag{3.1}$$

Equation (2.15) may then be written, for the lower and upper layers, as

$$\nabla^2\Psi = -A \tag{3.2}$$

with

$$A = R - \frac{\kappa_s}{\kappa}R_s \tag{3.3}$$

where R and R_S are Rayleigh numbers based on temperature and salinity, given by

$$R = \frac{\alpha g K_1 |\nabla T_d| H^2 \sin\gamma}{\kappa\nu} \tag{3.4}$$

$$R = \frac{\alpha_s g K_1 |\nabla T_d| H^2 \sin\gamma_s}{\kappa_s\nu} \tag{3.5}$$

Introducing a permeability contrast between the layers,

$$q = K_2/K_1 < 1 \tag{3.6}$$

equation (2.15) for the stream function in the middle layer may be written

$$\nabla^2\Psi = -qA \tag{3.7}$$

We notice from (3.2) - (3.5) that the condition that the fluid velocity be small in the upper and lower layers is that R and R_s are both small (or more specifically, the difference $R - \frac{\kappa_s}{\kappa}R_s$ is small). This means that either of the two angles γ and γ_s must be small, which is the case usually observed, or that $|\nabla T_d|$ and $|\nabla S_d|$ are small. For the special case where $\gamma = \gamma_s = \theta$, where θ is the angle the layers make with the horizontal, the temperature and salinity isolines are parallel to the strata. Since θ is not necessarily small, we then require that $|\nabla T_d| = \Delta T/H$ and $|\nabla S_d| = \Delta S/H$ have small values. Here ΔT

and ΔS are the absolute values of the differences between the temperature and salinity, respectively, at the upper and lower boundaries.

The streamlines can now be found from equations (3.2) and (3.7). Since the configuration is symmetric about the line $z = \frac{1}{2}H$, we need only consider the flow in the lower layer and half the middle layer. Assuming that the boundary at $z = 0$ is impenetrable, the following boundary conditions, in dimensional form, apply:

$$\psi = 0 \quad on\ z = 0 \tag{3.8}$$

$$w_z = 0 \quad on\ z = \tfrac{1}{2}H \tag{3.9}$$

$$\frac{u_1}{K_1} = \frac{u_2}{K_2},\ w_1 = w_2 \quad on\ z = rH \tag{3.10}$$

where the subscripts 1 and 2 refer to the lower and middle layers respectively. The boundary condition (3.9) reflects the symmetry, while (3.10) expresses continuity of pressure and vertical mass flux at the interface between layers 1 and 2. The ends of the slab at $x = 0$ and $x = L$ are assumed to be impenetrable:

$$\psi = 0 \quad on\ x = 0,\ L \tag{3.11}$$

The aspect ratio for the layered system, which later in the analyses will be assumed small, is given by

$$b = H/L \tag{3.12}$$

In non - dimensional form, the solutions may be given as the sum of a second order polynomial and an infinite Fourier series, as follows:

$$\Psi_1 = Ab^{-2}[\frac{1}{2}bX(1 - bX) + 4b^3 \sum_{n=0}^{\infty} B_n(Z)\sin(k_n X)] \tag{3.13}$$

$$\Psi_2 = Ab^{-2}[\frac{1}{2}qbX(1 - bX) + 4b^3 \sum_{n=0}^{\infty} C_n(Z)\sin(k_n X)] \tag{3.14}$$

which automatically satisfy the boundary conditions at the ends, which in non - dimensional coordinates are at $X = 0$ and $X = b^{-1}$. The Fourier series coefficients, determined from the boundary conditions (3.1)-(3.10) are given by

$$B_n(Z) = \frac{(1-q)[\cosh(k_n(\frac{1}{2}-r)\cosh[k_n(Z-r)] - \sinh k_n(\frac{1}{2}-r)\sinh(k_n Z)]}{k_n^3[q\cosh[k_n(\frac{1}{2}-r)]\cosh(k_n r) + \sinh[k_n(\frac{1}{2}-r)]\sinh(k_n r)]} - \frac{\cosh[k_n(Z-\frac{1}{2})]}{k_n^3[q\cosh[k_n(\frac{1}{2}-r)]\cosh(k_n r) + \sinh[k_n(\frac{1}{2}-r)]\sinh(k_n r)]} \tag{3.15}$$

$$C_n(Z) = \frac{q[1-(1-q)\cosh k_n r]\cosh[k_n(Z-\frac{1}{2})]}{k_n^3[q\cosh[k_n(\frac{1}{2}-r)]\cosh(k_n r) + \sinh[k_n(\frac{1}{2}-r)]\sinh(k_n r)]} \tag{3.16}$$

where

$$k_n = (2n+1)\pi b \tag{3.17}$$

4. The streamlines and velocity field

Values of the streamfunction are found by numerical summation of the series (3.16) and (3.16). The resulting streamlines for aspect ratio $b = 1$ and layer thickness ratio $\Delta H/H = 0.2$ and for permeability ratios $q = 1$, 0.35 and 0.05 are displayed in figures 4.1 (a), (b) and (c) respectively. It is observed that in the last case, where the permeability contrast is greatest, there is separation of the streamlines with a proportion of the fluid beeing resirculated within the layer. In the streamline figures (4.1 -4.4), the streamlines are labelled with the value of the dimensionless streamfunction multiplied with $100/A$.

In figure 4.2, the aspect ratio is the same as for figure 4.1, but now $\Delta H/H = 0.1$ and $q = 1$, 0.35, 0.05. Note that for the thinner middle layer, the permeability ratio, q must be smaller in order to obtain resirculation in the lower layer. This is further demonstrated in figure 4.3, where $b = 10^{-1}$, $\Delta H/H = 0.2$ and $q = 1$, 0.0038 and 0.0006, and in figure 4.4, where $b = 10^{-1}$, $\Delta H/H = 0.1$ and $q = 1$, 0.0038 and 0.0006. Where resirculation occur, the amount of fluid transported across the middle layer is reduced; in the present three - layer model, this reduction may be up to one half of the total flow.

It is of interest to find some necessary conditions for which resirculation whithin the lower layer occurs. To get more information about the velocity field, we have found expressions for the dimensionless velocity component u parallel to the layers; these formulae, valid for small values of the aspect ratio b and for flow which is not close to the endwalls, are derived analytically in the Appendix.

Far from the end boundaries, $U = \partial\psi/\partial Z$ is a function of Z only. In the lower layer,

$$U_1(Z) = -AZ + E_1(q/b^2, r) \tag{4.1}$$

where A is defined by (3.3) and E_1 is given in the Appendix. This formula is valid for all values of q. For sufficiently small values of b, then, the velocity parallel to the layers and far from the ends is a linear function of Z, and $\partial U/\partial Z$ $(= \partial^2\psi/\partial Z^2) = -A$; note from (3.2) that $\partial W/\partial X$ $(= -\partial^2\psi/\partial X^2)$ may then be neglected.

In the middle layer, we find that U is again a linear function of Z:

$$U_2(Z) = -A_2(Z - \frac{1}{2}) \tag{4.2}$$

where A_2, a function of q/b^2 and r, is defined in the Appendix. A_2 is generally not equal to the vorticity, qA. It may be shown from (A.19) in the Appendix that this is only so when $q/b^2 >> 1$, in which case $\partial W/\partial X$ is zero in the middle layer. Equation (4.2) may then be written

$$U_2(Z) = -qA(Z - \frac{1}{2}) \tag{4.3}$$

If q/b^2 is not large, $\partial W/\partial X$ is not zero even though b is very small. It follows from (A.19) that for small values of q/b^2, A_2 becomes negative, which is necessary for the separation of the streamlines and consequent resirculation in the sandstone layers.

Actually, equations (4.1) and (4.3) are readily generalized to be valid for an arbitrary variation of permeability $K(z)$, so that

$$U(Z) = -\frac{K(Z)}{K_1}AZ + constant \tag{4.4}$$

is valid for sufficiently small values of b. Equation (4.4) is easily derived from (2.3) by eliminating the pressure and assuming that $\partial W/\partial X$ is small.

Separation of the streamlines will occur when the fluid velocity at the central position $X = \frac{1}{2}b^{-1}$ is zero for some value of Z in the range $\frac{1}{2}r \leq Z \leq r$.It follows from (4.1) that, for small b, separation takes place when

$$E_1(q/b^2, r) = AZ \tag{4.5}$$

Note that the quantities which determine whether separation occurs or not are q/b^2 and r. The marginal values of these two quantities are obtained by setting $Z = r$.

For the general case where $b \leq 1$ but is not is not necessarily small, the strength of the resirculation in the lower layer may be measured by the elevation z_0 of the centre of the resirculation "roll". The marginal case is when $z_0 = r$, and total separation is given when the centre of the roll is in the middle of the lower layer i.e. $z_0 = \frac{1}{2}r$. We define a separation number ζ, defined by

$$\zeta = \frac{r - z_0}{\frac{1}{2}r} \tag{4.6}$$

Then, a value of $\zeta = 0$ gives marginal separation while $\zeta = 1$ represents total separation with flow completely resirculated in the lower layer and no flow through the middle layer (corresponding to $q = 0$). For given values of $r = \frac{1}{2}(1 - \Delta H/H)$ and separation number ζ, there is a unique relationship between q/b^2 and b, which can be be calculated numerically.

Two sets of examples for $\Delta H/H = 0.1$ and 0.2, corresponding to $r = 0.45$ and 0.40 respectively are displayed in figures 4.5 (a) and (b). In each of these figures, lines corresponding to ζ =0 (0.1) 0.9 are shown. It is seen that for $b < 0.1$, q/b^2 is independent of b. For small enough values of b, then, there is a unique relationship between q/b^2 and r for any given resirculation number ζ. This relationship is shown for $\zeta = 0$ and $\zeta = 0.5$ in figure 4.6. As expected, of course, as $r \to 0$ (the lower layer becoming infinitely thin), the criterion for resirculation is that $q/b^2 \to 0$.

In conclusion we note that for any small value of $q = K_2/K_1$, there will be no resirculation, and therefore no measurable effect of the thin middle layer on the convective flow in the slab, provided that the aspect ratio $b = H/L$ is sufficiently small. This is in contrast to the result for Rayleigh convection where thin layers with small permeability are effective in preventing the onset of convection (Bjørlykke, Mo & Palm, 1988).

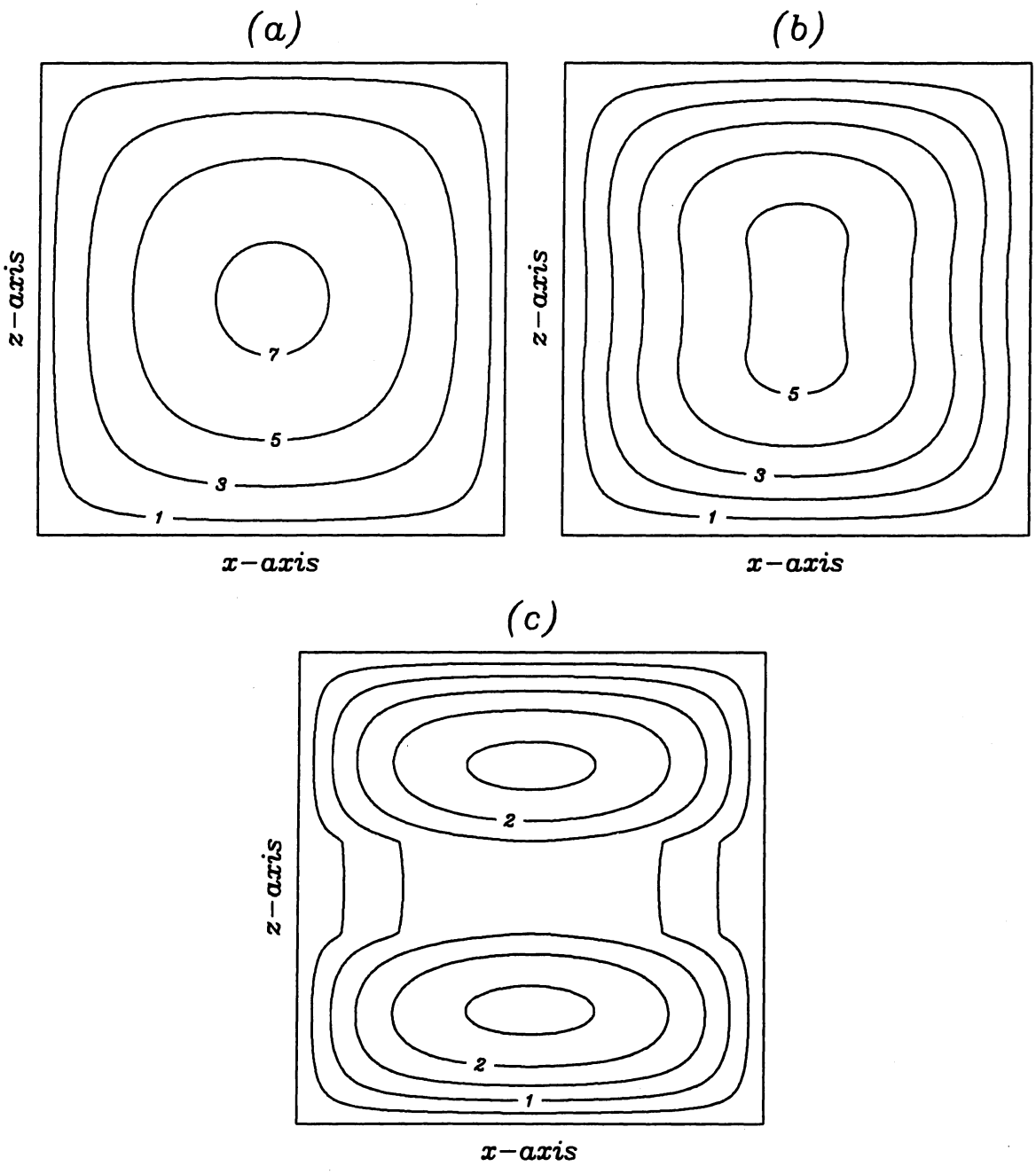

Figure 4.1: The streamlines for the aspect ratio $b = 1$, layer thickness ratio $\Delta H/H = 0.2$. (a) permeability ratio $q = 1$, (b) $q = 0.35$, (c) $q = 0.05$.

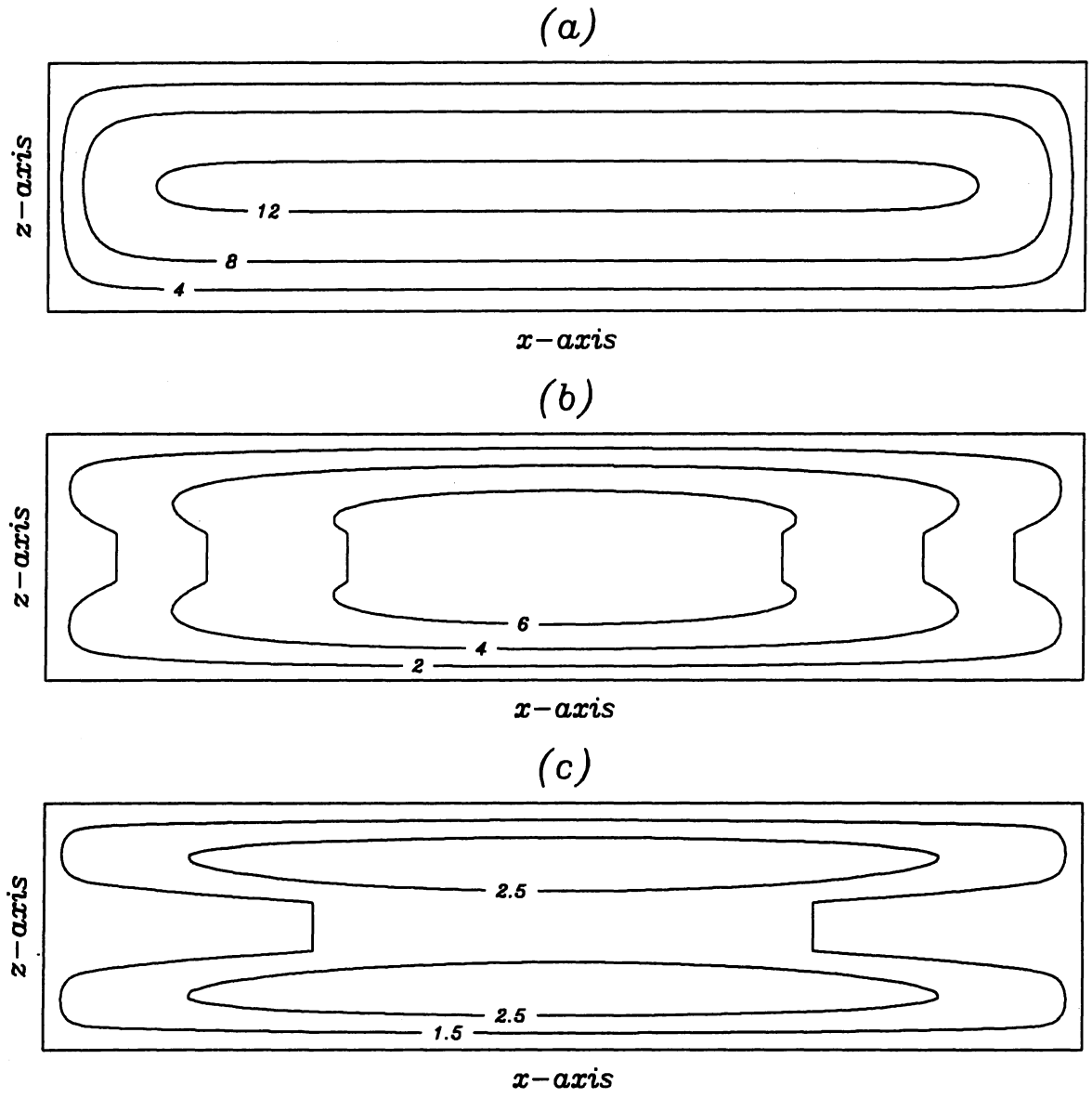

Figure 4.2: The streamlines for the aspect ratio $b = 0.1$, layer thickness ratio $\Delta H/H = 0.2$. (a) permeability ratio $q = 1$, (b) $q = 0.0038$, (c) $q = 0.0006$.

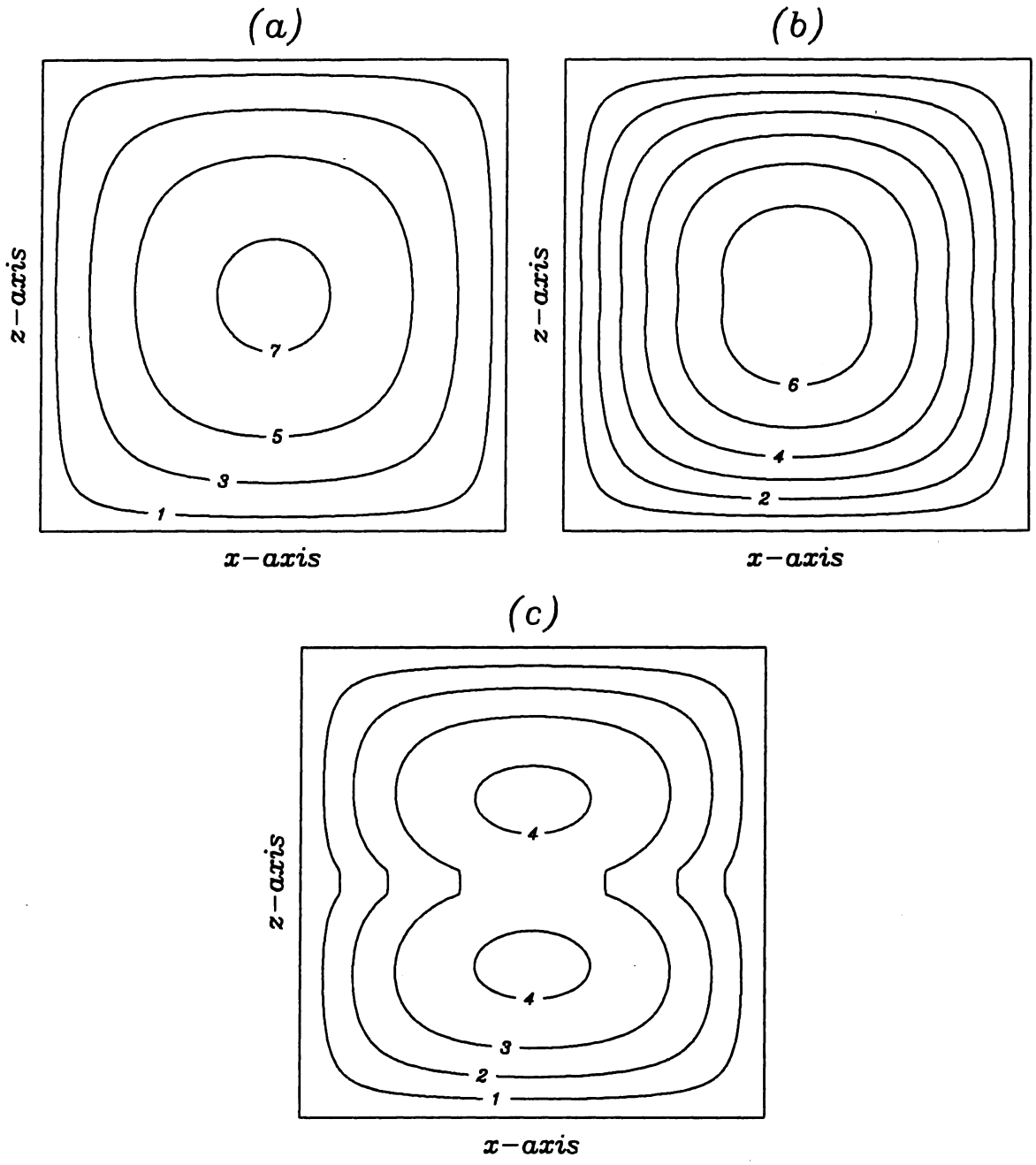

Figure 4.3: The streamlines for the aspect ratio $b = 1$, layer thickness ratio $\Delta H/H = 0.1$. (a) permeability ratio $q = 1$, (b) $q = 0.35$, (c) $q = 0.05$.

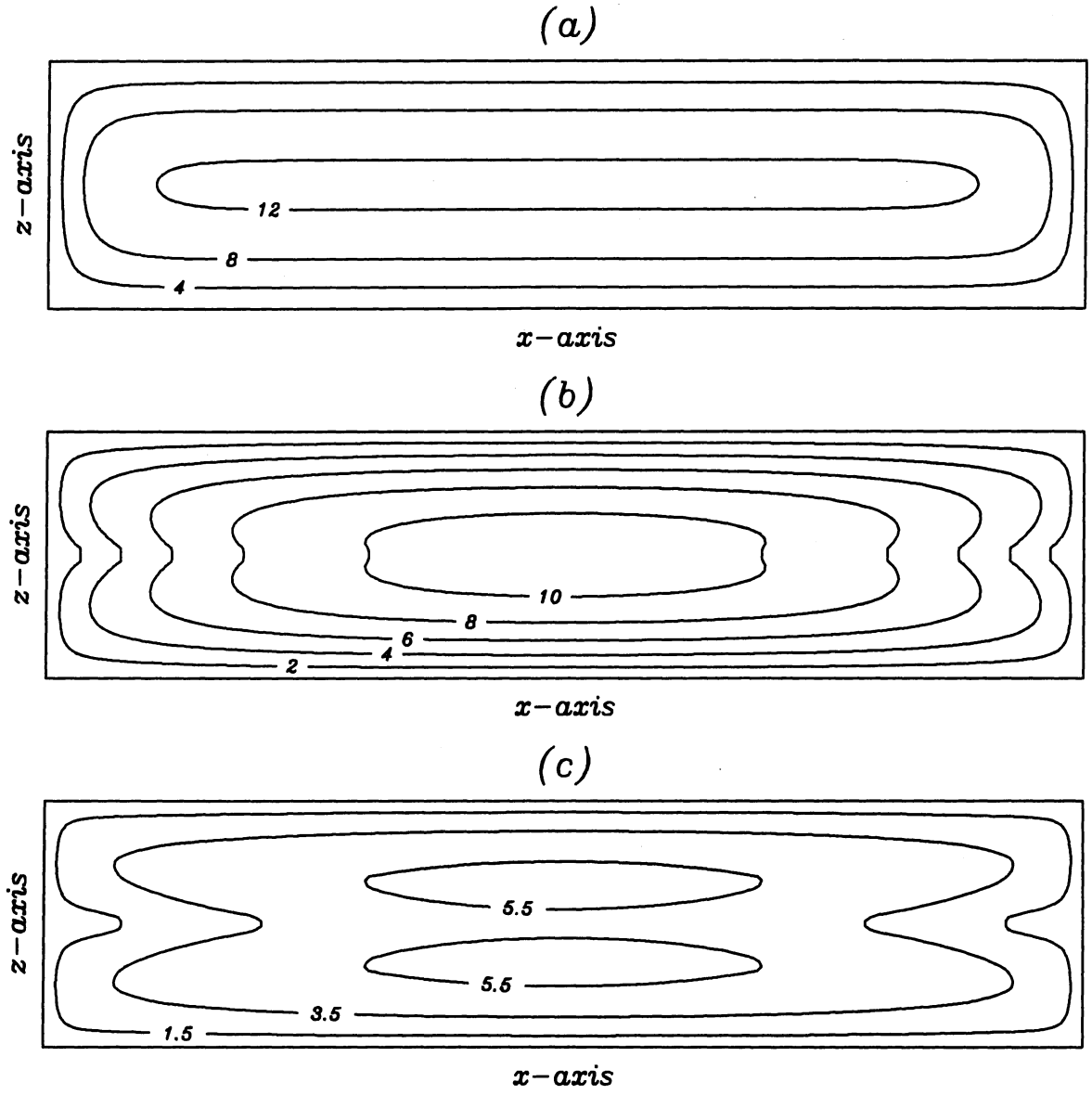

Figure 4.4: The streamlines for the aspect ratio $b = 0.1$, layer thickness ratio $\Delta H/H = 0.1$. (a) permeability ratio $q = 1$, (b) $q = 0.0038$, (c) $q = 0.0006$.

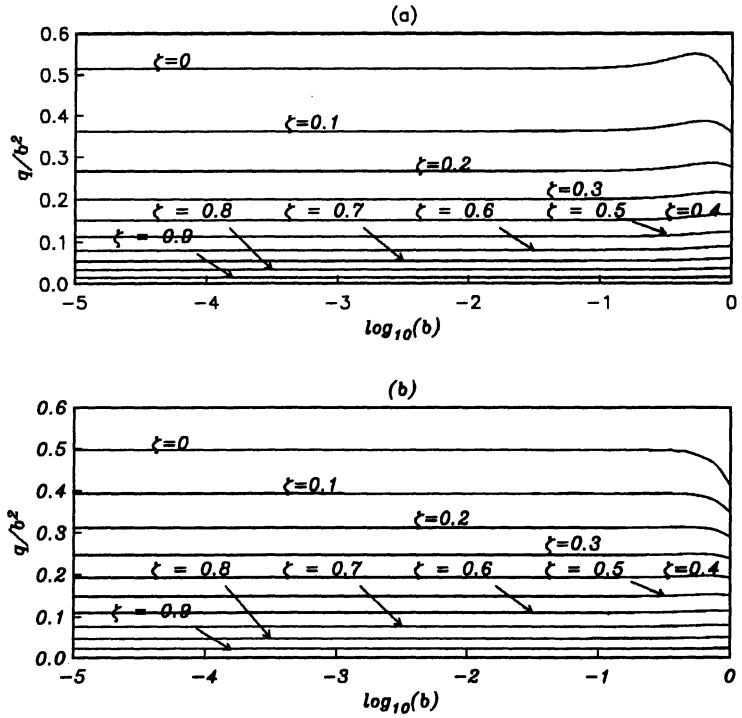

Figure 4.5: The values of q/b^2 for different degrees of separation. For the uppermost curve the separation number $\zeta = 0$ and is increasing downwards in the diagram by 0.1 for each curve. (a) $\Delta H/H = 0.1$, (b) $\Delta H/H = 0.2$.

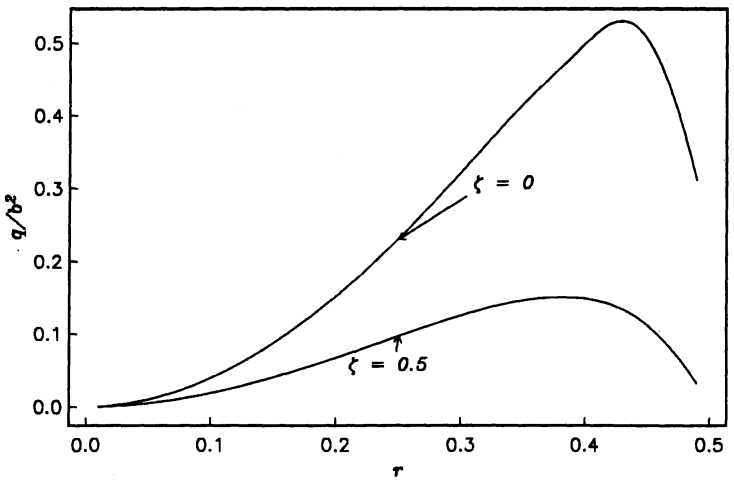

Figure 4.6: q/b^2 as function of $r = \frac{1}{2}(1 - \frac{\Delta H}{H})$ for $\zeta = 0$ and $\zeta = 0.5$.

5. Solute transport and change in porosity

Thermal convection in sloping porous layers where diagenetic processes are at work has been studied by Wood and Hewett (1982, 1984) and by Davis et al.(1985). They examined the mass transport of a soluble phase, associated with convective and diffusive action. It was assumed that the layer is composed of sandstone, that the solution is saturated and that the mechanism depends essentially only on temperature. For a material like quartz (silica) which has a solubility that increases with temperature, this means that material is leached from the porous matrix in regions where the fluid is heated and precipitated in regions where it is cooled. Davies et al. (1985) studied convection in a folded layer, embedded in an impermeable medium heated from below, whereas Wood and Hewett (1982, 1980) considered the mass transport in a single layer, bounded by parallel, sloping planes. They considered only the case where the isotherms are parallel to the sloping layer. However, as mentioned earlier in this work, this is not what is usually observed; rather the isotherms are aligned more horizontally than the geophysical strata.

Here, we shall use the results from the last section to examine the mass transport in some detail for various angles γ which the isotherms make with the horizontal. For simplicity, the effect of salt is ignored. Further, it has been shown in the last section above that, for sufficiently small values of the aspect ratio b, the effect of the middle layer may be disregarded. Thus we consider only a sloping one layer modell; the formulas (3.16) and (3.16) for ψ become identical and the problem is simplified.

The continuity equation for quartz may be written

$$\frac{\partial}{\partial t}[\rho_s(1-\phi)] = -\nabla\cdot(\rho c_s\vec{v}) + \phi D\nabla\cdot[\nabla(\rho c_s)] \tag{5.1}$$

where ρ_s is the density of the precipitated silica (quartz), ϕ is the porosity, c_s is the mass fraction of the dissolved silica, ρ and $\vec{v}$ are the density and Darcy velocity of the fluid (water) and D is the diffusion coefficient of silica in water.

Using the Boussinesque approximation as before, (5.1) can be rearranged

to the form

$$\frac{\partial \phi}{\partial t} = \frac{\rho_0}{\rho_s}(\vec{v} \cdot \nabla c_s - \phi D \nabla \cdot \nabla c_s) \tag{5.2}$$

We assume that the saturated concentration c_s is a function only of temperature. Writing

$$\left(\frac{\partial c_s}{\partial T}\right)_p = \frac{dc_s}{dT} \tag{5.3}$$

equation (5.2) may be written

$$\frac{\partial \phi}{\partial t} = \frac{\rho_0}{\rho_s}\frac{dc_s}{dT}\left(\vec{v} \cdot \nabla T - \phi D \nabla^2 T\right) - \frac{\rho_0}{\rho_s}\phi D \frac{d^2 c_s}{dT^2} \nabla T \cdot \nabla T \tag{5.4}$$

Using the notation from §2 above, and substituting $T = T_0 + T_d + T_s$, this last equation becomes

$$\frac{\partial \phi}{\partial t} = \frac{\rho_0}{\rho_s}\frac{dc_s}{dT}\left(\mathbf{v} \cdot \nabla T_d - \phi D \nabla^2 T_c\right) - \frac{\rho_0}{\rho_s}\phi D \frac{d^2 c_s}{dT^2} \nabla T_d \cdot \nabla T_d \tag{5.5}$$

Here, $\vec{v}$ is the velocity due to the diffusion temperature distribution and higher order products of the small quantities, $\vec{v}$, ∇T_d and ∇T_c are neglected. Also $\nabla^2 T_d = 0$ from (2.11). Now, from (2.4)

$$\mathbf{v} \cdot \nabla T_d = \kappa \nabla^2 T_c \tag{5.6}$$

Here, $\kappa = o(10^{-6})$ while $D = o(10^{-9})$; hence the second term in (5.5) may be neglected compared with the first.

The saturation concentration $c_s(T)$ is approximated well for $273 < T < 523$ (see, for example, Fournier, 1985) by

$$log_{10}(c_s) = 5.19 - \frac{1309}{T} \tag{5.7}$$

where T is given in Kelvin. For $T = 373K$,

$$c_s = 47.7 \cdot 10^{-6}, \quad \frac{dc_s}{dT} = 1.1 \cdot 10^{-6} K^{-1}, \quad \frac{d^2 c_s}{dT^2} = 1.7 \cdot 10^{-8} K^{-2} \tag{5.8}$$

Using typical values of

$$|\nabla T_d| = 0.03 K m^{-1}, \quad \phi = 0.3, \quad \frac{\rho_0}{\rho_s} = \frac{1}{2.6} \tag{5.9}$$

the diffusion term becomes

$$\frac{\rho_0}{\rho_s}\phi D \frac{d^2 c_s}{dT^2}(\nabla T_d)^2 = 1.8 \times 10^{-21} s^{-1} \tag{5.10}$$

It is reasonable for comparison to let thermal convection effect (first term in (5.6)) be represented by, in turn, both the convection far from the boundaries,

where $w = 0$, and convection at the end walls, where $u = 0$, since one of these terms may be very small, or zero, for some combination of layer and isotherm angles. From (2.15) the velocity parallel to the layer far from the end boundaries

$$u = -\frac{\alpha g K}{\nu}|\nabla T_d|\left(z - \frac{1}{2}H\right)\sin\gamma \tag{5.11}$$

The maximum value u_{max} is given at the lower boundary $z = 0$. It may be shown, by expressing the solution of (2.15) as a polynomial in z (instead of x, as detailed above) and a Fourier series, that the maximum value w_{max} of w at the end walls is given at $z = \frac{1}{2}H$ and is related to u_{max} by

$$w_{max} = 0.74 u_{max} \tag{5.12}$$

Details of the calculation are straightforward and are not given here.

We introduce characteristic values of the various parameters as follows:

$$\alpha = 7.1 \times 10^{-4} K^{-1} \quad \nu = 3 \times 10^{-1} m^2 s^{-1} \tag{5.13}$$

$$g = 9.8 m s^{-2} \qquad H = 30m \tag{5.14}$$

Then, from (5.11) and (5.12),

$$u_{max} = 1.1 \times 10^4 K \sin\gamma \; m s^{-1} \tag{5.15}$$

$$w_{max} = 0.8 \times 10^4 K \sin\gamma \; m s^{-1} \tag{5.16}$$

Further,

$$\frac{\partial T}{\partial x} = -|\nabla T_d| \sin(\theta - \gamma) \tag{5.17}$$

and

$$\frac{\partial T}{\partial z} = -|\nabla T_d| \cos(\theta - \gamma) \tag{5.18}$$

Note that the velocity field is independent of layer angle θ, whereas the temperature gradients (5.17) and (5.18) depend on the relative orientation of the layer and the isotherm slopes.

Choosing, first, $\theta = 15^0$, and using the parameter values given in (5.9) and (5.14), we obtain:

$$K^{-1}\frac{\rho_0}{\rho_s}\frac{dc_s}{dT}u\frac{\partial T}{\partial x} = \; 5.7 \times 10^{-7}, 1.5 \times 10^{-6}, 2.0 \times 10^{-6}, 0 \tag{5.19}$$

$$K^{-1}\frac{\rho_0}{\rho_s}\frac{dc_s}{dT}w\frac{\partial T}{\partial x} = \; 1.7 \times 10^{-6}, 5 \times 10^{-6}, 1.7 \times 10^{-5}, 2.6 \times 10^{-9} \tag{5.20}$$

for $\gamma = 1^0$, 3^0, 10^0 and 15^0 respectively. For $\theta = 30^0$, the values are:

$$K^{-1}\frac{\rho_0}{\rho_s}\frac{dc_s}{dT}u\frac{\partial T}{\partial x} = \; 1.1 \times 10^{-6}, 3.3 \times 10^{-6}, 9.4 \times 10^{-6}, \; 0 \tag{5.21}$$

$$K^{-1}\frac{\rho_0}{\rho_s}\frac{dc_s}{dT}w\frac{\partial T}{\partial x} = \ 1.5\times10^{-6}, 4.7\times10^{-6}, 2.5\times10^{-5}, 5.1\times10^{-5} \quad (5.22)$$

for $\gamma = 1^0$, 3^0, 10^0, 15^0 and 30^0 respectively.

Comparison with the value of the diffusion term (5.10) shows that the thermal convection effect domminates over diffusion when the permeability K is larger than about 0.1 *darcy* ($0.1\times10^{-12}m^2$). The diffusion term is henceforth neglected. Equation (5.5) then reduces to

$$\frac{\partial\phi}{\partial t} = -\frac{\rho_0}{\rho_s}\frac{dc_s}{dT}|\nabla T_d|[u\sin(\theta-\gamma)+w\cos(\theta-\gamma)] \quad (5.23)$$

The velocity components u and w can be found (with suitable redimensionalisation) from (3.13) and (3.14) with $q = 1$. The streamline field corresponding to $b = 0.1$ is shown in figure 4.3 (a).

For a relatively short span of time we may integrate (5.23) considering u and w to remain constant for the duration. Then

$$\phi(t) = \phi(0) + \frac{\partial\phi}{\partial t}t \quad (5.24)$$

where $\phi(0)$ is the porosity at $t = 0$.

It is easily shown that the maximum change of the porosity takes place at a point at the boundary of the porous slab. We first note that it follows from (5.23) that $\partial\phi/\partial t$ has a maximum at the point where $u\sin(\theta-\gamma)+w\cos(\theta-\gamma)$ attains its maximum. Now

$$\begin{aligned} u\sin(\theta-\gamma)+w\cos(\theta-\gamma) &= \vec{v}\cdot\vec{c} \\ &= (\vec{k}\times\nabla\psi)\cdot\vec{c} = (\vec{c}\times\vec{k})\cdot\nabla\psi \quad (5.25) \\ &= \vec{s}\cdot\nabla\psi = \frac{\partial\psi}{\partial s} \quad (5.26) \end{aligned}$$

where $\vec{c}$ is the constant unit vector

$$\vec{c} = (\sin(\theta-\gamma), \cos(\theta-\gamma)) \quad (5.27)$$

$\vec{k}$ is the unit vector perpendicular to the (x,z) plane and $\vec{s}$ is a constant unit vector perpendicular to both $\vec{c}$ and $\vec{k}$. $\partial\psi/\partial s$ denotes the derivative along $\vec{s}$. From (3.2) we obtain, by differensiation with respect to s,

$$\nabla^2\frac{\partial\psi}{\partial s} = 0 \quad (5.28)$$

According to a fundamental result in mathematics, every function which satisfies the Laplace equation has its extremum values on the boundaries; this proves the statement.

The extremum points must be located either at the mid - points of the end walls ($x = 0,\ L$; $z = H/2$) or at the mid - points of the lateral boundaries

$(x = L/2;\ z = 0,\ H)$. It follows from (5.12) and (5.23) that the extremum points of $\partial\phi/\partial t$ are located at the mid - points of the endwalls if $\theta - \gamma < 36.5^0$ and at the mid - points of the lateral boundaries if $\theta - \gamma > 36.5^0$.

Examples following the calculation of porosity changes given by (5.24) are given for an initial porosity $\phi(0) = 0.3$, a permeability $K = 1Darcy(10^{-12}m^2)$ and a slab thickness $H = 30m$. Figure 5.1 shows the change in porosity throughout the layer at a time τ which corresponds to a change of 10% of its initial value at the end - point. In figure 5.1 (a), $\gamma = 1^0$ and $\theta = 15^0$; τ is found to be 5.7×10^8 years. In figure 5.1 (b), where $\gamma = 3^0$ and $\theta = 15^0$, $\tau = 1.9 \times 10^8$ years whereas in figure 5.1 (c), $\gamma = \theta = 15^0$ and $\tau = 3.7 \times 10^7$ years. In the last case, the convective effect is noticeable only near the end boundaries.

In figure 5.2, $\gamma = 3^0$ and $\theta = 40^0$. τ is now the time which corresponds to a change of 10% of its initial value at the mid - points of the lateral boundaries. In this case, τ is found to be 2.2×10^8years.

In figure 5.3, the thermal conductivity of the sandstone layer is larger than that of the surrounding rock $(k/k_s > 1)$ so that γ is negative. γ is chosen to be -10^0 and $\theta = 30^0$, which gives $\theta - \gamma = 40^0$. τ is now found to be 6.4×10^7 years.

Note that in figure 5.1, where $\theta - \gamma < 36.5^0$, the changes in porosity are much more rapid at the end walls than far from the ends. In figures 5.2 and 5.3, however, where $\theta - \gamma > 36.5^0$, the changes are most rapid at the lateral boundaries far from the ends.

Note also, from figures 5.2 and 5.3, that if the thermal conductivity for sandstone is larger than that of the bounding rock, the porosity will <u>increase</u> with time at the lower boundary, whereas the porosity will <u>decrease</u> with time at this boundary if the conductivity for sandstone is smaller than that of the surrounding rock.

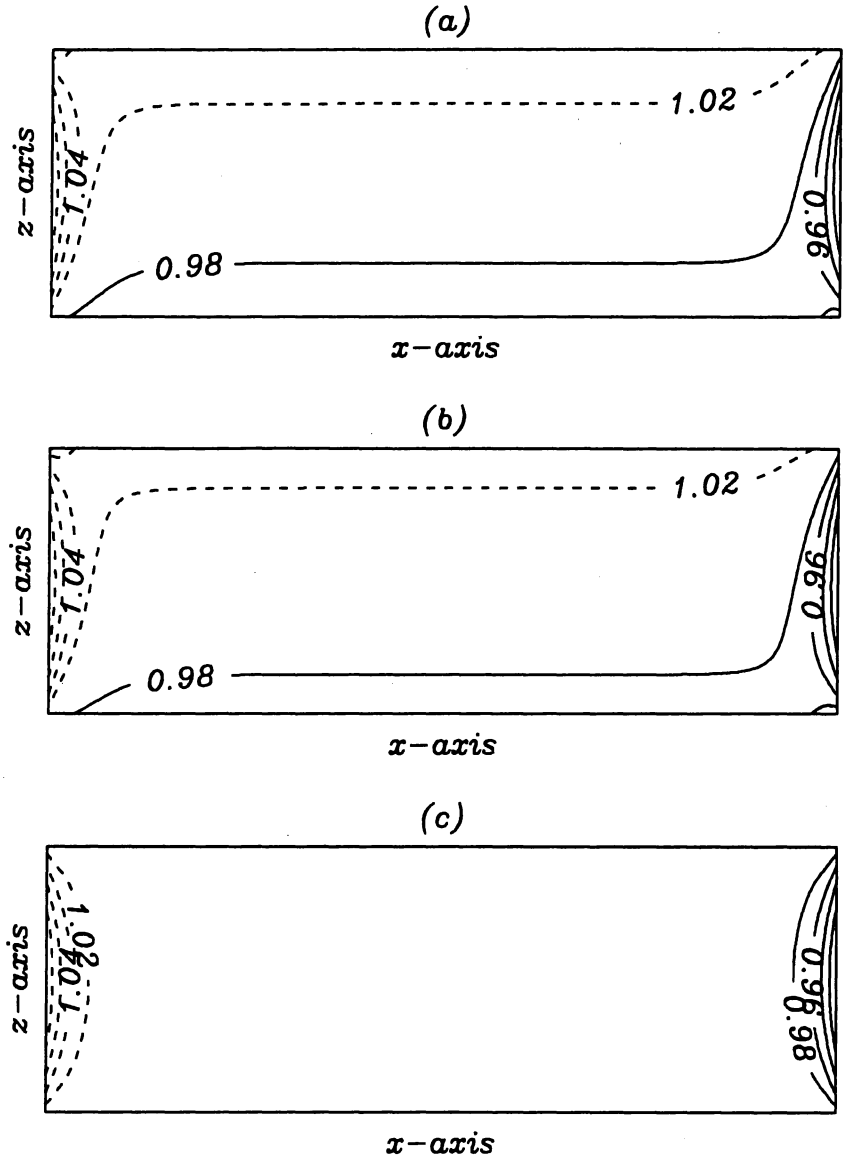

Figure 5.1: Curves of constant porosity at a time τ which corresponds to a change of 10% of its initial value at the end - points. The aspect ratio $b = 0.1$ and $\theta = 15^0$. (a) $\gamma = 1^0$, (b) $\gamma = 3^0$, (c) $\gamma = 15^0$.

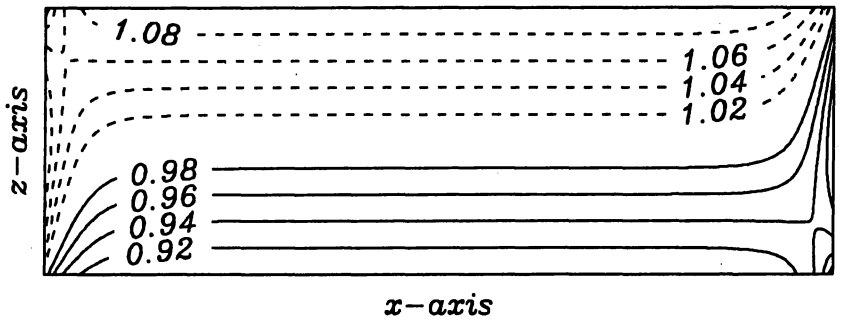

Figure 5.2: Curves of constant porosity at a time τ which corresponds to a change of 10% of its initial value at the mid - points of the lateral boundaries. The aspect ratio $b = 0.1$, $\gamma = 3^0$ and $\theta = 40^0$.

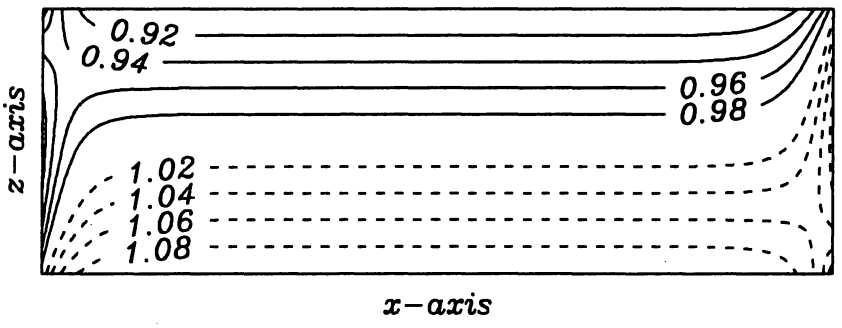

Figure 5.3: The same as figure 9, but $\gamma = -10^0$ and $\theta = 30^0$. Note that for γ negative, the sign of the change in porosity is changed.
aspect ratio 0.1 and slope angle 30^0.

6. Summary and conclusions

This paper is concerned with convection in sloping layers of sandstone, caused by non - horizontal isolines of water density which is assumed to be a function of temperature and salinity. The layered, porous slab is assumed to make an angle θ, the isotherms an angle γ and the isolines of salinity an angle γ_s with the horizontal and these angles may be different. The first part of the work consideres a three - layer model consisting of two identical sandstone layers separated by a thin (shale) layer of low permeability. The overall aspect ratio $b = H/L$ (see figure 1.1) is small.

The calculated flow field shows strong dependence on the value of the dimensionless parameter q/b^2, where $q = K_2/K_1$ is the ratio of the permeabilities of the shale and sandstone layers respectively. If q/b^2 is of order unity or smaller, flow resirculation will occur within the sandstone layers. If q/b^2 is much larger than unity, the shale layer has little practical effect on the flow and no resirculation takes place. So for given values of K_1 and K_2 (K_2 may be much smaller than K_1) the flow will not notice thin shale layers if the aspect ratio b is sufficiently small.

For small aspect ratio, the flow in the sandstone layers far from the ends is characterized by the velocity u in the $x-$ direction (see figure 1.1) being a linear function of z, and $\partial w/\partial x$, where w is the velocity in the z - direction, is very small. The velocity u in the shale layer is also a linear function of z, but if the value of q/b^2 is moderate or small, so that resirculation occurs, $\partial w/\partial x$ cannot be neglected in that layer even though the aspect ratio is very small. It is then necessary to take the endwalls into account. When resirculation does not occur (q/b^2 large), $\partial w/\partial z$ can also be neglected in the shale layer.

It is also shown that the slope of the isotherms, $\tan\gamma$, is determined by $\tan\theta$ and k/k_s where k and k_s are the thermal conductivities of the slab and boundary rock, respectively.

Results of calculations of the spatial variation of porosity changes due to the flow over small values of time are given in the last paragraph of section 5. The model in that section is simplified to a single layer and salinity effects are neglected. It is shown that the maximum change in porosity always takes place at the boundary of the layer. Furthermore, if $\theta - \gamma$ is less than 36.5^0, the maximum change takes place at the middle points of the endwalls ($x = 0,\ L;\ z = H/2$). If $\theta - \gamma$ is greater than 36.5^0, the maximum change

occurs at the middle points of the lateral boundaries ($x = L/2;\ z = 0,\ H$). The time it takes for a change of 10% in porosity at the maximum points depends very much on γ, θ, the thickness of the layer H, and the permeability K. We have chosen $H = 30m$ and K=1 Darcy. We then find, for $\theta = 15^0$ and γ varying from 1^0 to 15^0, that the time varies from 5.7×10^8 years to 3.7×10^7 years. The time is inversely proportional to the permeability and the slab thickness. If K is kept constant and H is increased to $300m$, the necessary time is reduced to 1/10 of the values given above.

It is seen from the figures 5.1 that for $\theta - \gamma$ less than 36.5^0, the changes in porosity take place mainly at the endwalls and are therefore difficult to observe. For $\theta - \gamma > 36.5^0$, large changes occur at the lateral boundaries over large distances and should therefore be easier to detect.

If γ is negative, which correspond to the thermal conductivity of the sandstone being larger than that of the surrounding rock, the porosity will increase with time at the lower boundary and decrease with time at the upper boundary. If γ is positive, the porosity will decrease at the lower boundary and increase at the upper boundary.

Acknowledgement

This research has been supported by VISTA, a research cooperation between the Norwegian Academy of Science and Letters and Den Norske Stats Oljeselskap (Statoil). The authors also thank Professor Knut Bjørlykke for useful comments and suggestions.

Appendix A

Asymptotic values of the velocity parallel to the layers.

The nondimensionalised velocity component $U(X,Z)$ parallel to the layers, found from (3.13) and (3.14) for the lower and middle layer respectively, is given by

$$U_1 = \frac{\partial \Psi_1}{\partial Z} = 4Ab \sum_{n=0}^{\infty} B_n'(Z) \sin k_n X \tag{A.1}$$

$$U_2 = \frac{\partial \Psi_1}{\partial Z} = 4Ab \sum_{n=0}^{\infty} C_n'(Z) \sin k_n X \tag{A.2}$$

where

$$B_n'(Z) = \frac{1-q}{D}\left[\cosh k_n(\frac{1}{2}-r)\sinh k_n(Z-r) - \sinh k_n(\frac{1}{2}-r)\cosh k_n Z\right] - \sinh k_n(Z-\frac{1}{2}) \tag{A.3}$$

$$C_n'(Z)\frac{q}{D}\left[1-(1-q)\cosh k_n r\right]\sinh k_n(Z-\frac{1}{2}) \tag{A.4}$$

where

$$D = k_n^2\left[q\cosh k_n r \cosh k_n(\frac{1}{2}-r) + \sinh k_n r \sinh k_n(\frac{1}{2}-r)\right] \tag{A.5}$$

We want to examine U far from the end boundaries, so choose $X = b^{-1}/2$. Equations (A.1) and (A.2) then reduce to, respectively,

$$U_1 = U_1(Z) = 4Ab\sum_{n=0}^{\infty}(-1)^n B_n'(Z) \tag{A.6}$$

$$U_2 = U_2(Z) = 4Ab\sum_{n=0}^{\infty}(-1)^n C_n'(Z) \tag{A.7}$$

We split the sums in (A.6) and (A.7) into two parts:

$$\sum_{n=0}^{\infty} = \sum_{n=0}^{N} + \sum_{n=N}^{\infty} \tag{A.8}$$

where N is to be chosen so that amongst other criteria to be outlined below, $k_N = (2N+1)\pi b$ is small. Since N is large, this means that b must be sufficiently small.

We now consider (A.6) and find an upper bound for the second sum from $N+1$ to ∞. The term $B_n'(z)$ given by (A.3) has three parts, determined by the three terms in the numerator. Note that the denominator D, given by $A.5$ is always positive. The first part of $B_n'(z)$ is negative for all n. The absolute value of the alternating series is bounded:

$$|4Ab \sum_{n=N+1}^{\infty} (-1)^n \frac{(1-q)\cosh k_n(\frac{1}{2}-r)\sinh k_n(Z-r)}{D}| \quad \text{(A.9)}$$

$$< 4Ab\frac{(1-q)\cosh k_{N+1}(\frac{1}{2}-r)\sinh k_{N+1}(Z-r)}{D(k_{N+1}} < 4Ab\frac{1-q}{q}\frac{1}{k_{N+1}^2}$$

Correspondingly, the second series is also bounded by $4Ab(1-q)/qk_{N+1}^2$. The third part gives a contribution which is less in absolute value than $1/qk_{N+1}^2$. Hence

$$\Delta = |4Ab\sum_{N+1}^{\infty}(-1)^n B_n'(z)| < \frac{4Ab[2(1-q)+1]}{qk_{N+1}^2} < \frac{A[2(1-q)+1]}{q\pi^2}\frac{1}{bN^2} \quad \text{(A.10)}$$

upon using $k_n = (2n+1)\pi b$ from (3.17).

The value of N is now chosen so that the remainder Δ may be arbitrary small. That this can be done without violating the condition that k_n be small by setting

$$b = O(\delta), \quad N = O(\delta^{-1+\beta}) \quad \text{(A.11)}$$

We then have

$$\frac{1}{bN^2} = O(\delta^{1-2\beta}) \quad \text{(A.12)}$$

and

$$k_N = O(Nb) = O(\delta^{\beta}) \quad \text{(A.13)}$$

Both are small when $\delta \to 0$, provided that $0 < \beta < 0.5$.

The velocity parallel to the layers may therefore be approximated by

$$U_1 = 4Ab\sum_{n=0}^{N}(-1)^n B_n'(z) \quad \text{(A.14)}$$

where, for a given value of b, N is chosen so that k_N is small. We may now expand $B_n'(z)$ in a series of k_n, for small values of b, it suffices to include only the first term in the expansion. After some simple algebra, we obtain

$$U_1(z) = D_1 Z + E_1 \quad \text{(A.15)}$$

where

$$D_1 = -\frac{4A}{\pi}\sum_{n=0}^{N}(-1)^n\frac{1}{2n+1} \quad \text{(A.16)}$$

and

$$E_1 = \frac{4A}{\pi}\sum_{n=0}^{N}(-1)^n \frac{1}{2n+1}\frac{\frac{1}{2\pi^2}\frac{q/b^2}{(2n+1)^2}+\frac{1}{2}r^2(\frac{1}{2}-r)}{\frac{1}{\pi^2}\frac{q/b^2}{(2n+1)^2}+r(\frac{1}{2}-r)} \tag{A.17}$$

Since N is large, the sum in (A.16) may be replaced by a sum from zero to infinity; then we obtain

$$D_1 = -A \tag{A.18}$$

The corresponding velocity in the middle layer is

$$U_2(z) = -\frac{4A}{\pi}\sum_{n=0}^{N}(-1)^n \frac{1}{2n+1}\frac{\frac{1}{\pi^2}\frac{q/b^2}{(2n+1)^2}-\frac{1}{2}r^2}{\frac{1}{\pi^2}\frac{q/b^2}{(2n+1)^2}+r(\frac{1}{2}-r)}(Z-\frac{1}{2}) = -A_2(Z-\frac{1}{2}) \tag{A.19}$$

Note that for small b, E_1 and A_2 are functions only of q/b^2 and r.

Bibliography

[1] Bjørlykke, K., Mo, A. and Palm, E. (1988). Modelling of thermal convection in sedimentary basins and its relevance to diageneticreactions. *Marine Petr. Geol., pp 338-351.*

[2] Bories, S.A. and Combarnous, M.A. (1973). Natural convection in a sloping porous layer. *J.Fluid Mech. pp 63 - 79*

[3] Davis, S.H., Rosenblat, S., Wood, J.R. and Hewett, T.A. (1985). Convective fluid flow and diagenetic patterns in domed sheets. *Am.J.Sci., pp 707 - 777.*

[4] Fournier, R.O. (1985). The behaviour of silica in hydrothermal solutions. *In Reviews in Economic Geology 2, pp 45 - 61.*

[5] Palm, E. (1990). Rayleigh convection, mass transport and change in porosity in layers of sandstone. *J. Geophys. Res. 95, No. B6, pp 8675 - 8679.*

[6] Wood, J.R. and Hewett, T.A. (1982). Fluid convection and mass transfer in porous sandstones - a theoretical model. *Geochim. Cosmochim. Acta 46, pp 1707 - 1713.*

[7] Wood, J.R. and Hewett, T.A. (1984). Reservoir diagenesis and convective fluid flow. In McDonald, D.A. and Surdam, W.C. (eds) Clastic diagenesis. *Am. Assoc. Petrol. Geol. Memoirs 21, pp 99 - 111.*